

Mathematical Modelling Of Malaria Disease In Busia County, Kenya

Mogambi Nyasuguta Lucy¹, Dr. Mary Opondo²

School Of Pure And Applied Sciences, Kenyatta University, Box 43844-00100, Nairobi, Kenya

Abstract:

Background: Millions of people throughout the world die every year from malaria, an illness spread by the bite of an infected female *Anopheles* mosquito. Busia, a county in Kenya, has been recorded to have the highest prevalent cases of 37% in Kenya. However, Busia has often been ignored in the mathematical modelling of malaria in Kenya. The SEIR model is widely used in mathematical simulations of malaria transmission. However, the paradigm is no longer relevant to malaria cases since asymptomatic *Plasmodium* parasites persist in the systems of persons who have recovered from malaria. In this study, the human subpopulation carrying the *Plasmodium* parasites but are not suffering from malaria are included in the mathematical model. Therefore, this study presents SIRSp model to study the trend of malaria disease in Busia County, Kenya. The mathematical model is analysed in the human population by assuming that the disease's infection rate is constant and is based not only on the number of people who are infected but also on the number of people who are susceptible to the disease. The reproduction number in human and in mosquitoes are obtained and the equilibrium point shows that the disease-free equilibrium point is always stable. This suggests the possibility of eradicating malaria in Busia County. From the numerical simulations, it is found out that the infected humans increase with the force of infection. Increase in the rate of recovery from malaria reduces the number of infected humans and the infectious mosquito subpopulation but increases the susceptible human subpopulation.

Methodology:

The stability of the system is established and it shows that the system is always stable when the subpopulations start in the neighbourhood of the disease-free equilibrium point. The numerical solution of the system is sought using an adaptive step-size Runge-Kutta-Fehlberg (RKF45) method. The parameter estimation was carried out by using the Broyden-Fletcher-Goldfarb-Shanno (BFGS) method and the optimal parameter values are obtained as; $\Lambda_h = 1, \gamma = 1, \alpha = 1, r = 0.39195362, \Lambda_m = 1, \beta = 1, \mu_m = 0, p = 0.72426444, q = 0.23809668$.

Optimisation of the parameters is done by comparing the numerical results with the real-world data. The optimal parameter values are obtained as; $\Lambda_h = 1, \gamma = 1, \alpha = 1, r = 0.39195362, \Lambda_m = 1, \beta = 1, \mu_m = 0$. To show the fitting of the optimal values against the real-world data, we plotted the graphs.

Results and Conclusions: In this model the parameters are optimised and predicted the rate of human infection, the rate at which mosquitoes get infected and the rate at which human beings recover. The results shows that an increase in the rate of recovery of an infected human reduces the infection in the human population. The optimised model for the infected human subpopulation agrees well with the real-world data as time proceeds.

Keywords: Malaria transmission, Reproduction number, parameter optimisation and stability.

Date of Submission: 14-02-2024

Date of Acceptance: 24-02-2024

I. Introduction

Malaria is a widespread infectious disease caused by parasites of protozoan recognized as *Plasmodium* where blood cells are infected by parasite and replicated (Cai *et al.*, 2017). It is spread among humans occasioned by a bite of female adult *Anopheles* mosquito which is infected that exist as a *Plasmodium* of five species namely: *falciparum*, *vivax*, *ovale*, *malariae* and *knowlesi* (Lashari *et al.*, 2012). On the same breath, WHO (2019) reports that among these species, *P. falciparum* is the most severe and potentially lethal to humans while Cai *et al.* (2017) affirms that *P. falciparum* is the cause for high number of deaths, clinical cases and widespread among the tropical regions and subtropical regions. Based on Ahmed *et al.*, (2022) mosquito bite infections show some medical symptoms such as body temperature rise, pain, fatigue, sweat and shivering which may exist within five hours. Also, critics argue that malaria control has ineffective anti-malaria drugs and low efforts to develop effective vaccine to counter the resistance evolved in the parasite (Lashari *et al.*, 2012).

Based on recent report on World malaria by WHO (2021), 241 million malaria cases were observed in 2020 as related to 227 million in 2019. The number of estimated demises were 627000 in the year 2020; an increment of 69000 over the previous year. The study shows there were 95% malaria cases and 96% deaths in Sub-Saharan Africa. Among the deaths, 80% accounted for under 5 years of age children (WHO, 2021). The severity of malaria infection depends largely on the person's immune system of the infected person, fractional immunity progresses over a period through recurrent contagion and if the infection is not recurrent, the immunity becomes relatively short-lived. Being infected with the parasite does not automatically upshot in the disease. Numerous infected individuals in regions prevalent to malaria are asymptomatic: they may dock huge records of parasites yet display no superficial symbols and symptoms of the disease. The epidemiology of malaria broadcast and its degree of infection vary in different areas due to variability of weather conditions.

The World Health Organization (2019) has incorporated strategies for controlling and eliminating the spread of malaria. Mathematically, modelling has been a vital tool for manipulating choice creation procedures concerning intrusion plans towards curbing the spread of the disease. Recommending one intervention is ineffective to stem the blowout of malaria in a particular population for example, in places where *P. vivax* is the prevalent species, the use of insecticide-treated nets (ITN) and indoor residual spraying (IRS) may be less efficient at preventing the spread of the disease because mosquitoes often bite early in the evening, consume blood meals, and rest outside (WHO, 2019).

Health sector in Kenya has placed significant efforts in combatting the outbreak of malaria in Kenya and with the aim of reducing death from malaria by 75 per cent (Elnour et al., 2023). However, according to Bashir et al. (2019), majority of the Busia County population is susceptible to malaria due to poverty and insufficient health facilities. Busia County accounts for the largest malaria cases in Kenya. Malaria spread is extremely flexible in Busia County due to the varying climatic conditions. Malaria exists in four epidemiological zoning in Kenya: seasonal malaria transmission, malaria-free zones malaria endemic locations and malaria epidemic prone areas (WHO, 2019). These encounters call for crucial expansion of real and ideal policies for averting and regulating the spread of malaria. To overcome malaria in Kenya is therefore tantamount to overcoming it in Busia County. This study develops an appropriate SIRS_p model to identify the trend and patterns in the outbreak of Malaria in Busia County of Kenya.

II. Literature Review

The mathematical modelling of mosquito disease proves to avail appropriate strategies in the undercurrents of spread and insights in the control measures (Banerjee and Sanyal, 2023). Based on sir Ross model, malaria disease modelling was grounded on malaria life cycle parasite (Amadi and Haario, 2021). The model is further modified in other literatures to cover the infection latent period, factors for immunity, heterogeneous human and mosquito, susceptible population, exposure of both human and mosquito and human recoveries (Lashari et al., 2012; Cai et al., 2017; Cai et al., 2019).

Globally, malaria control among travellers was modelled through a mathematical model of SEIR by Olaniyi et al. (2020) while Ibrahim et al. (2020) enhanced awareness techniques in control of malaria transmission through SEIR model. Also, how the malaria parasite transmits from person to person was studied by Baihaqi et al., 2020, who suggested the SEIRS_p model by introducing a new compartment S_p in human population i.e. the susceptible with plasmodium parasite in the human body which relapses once the immunity decreases. Consequently, Djidjou-Demasse et al., 2020 developed an SEIR study model of the malaria disease spread and its effects on weather parameters. Similarly, Pandey (2020) offered a mathematical model to designate the role played by domestic and industrial effluents in malaria dispersal of malaria whereas, Song et al., 2020 familiarized with a mathematical model for malaria-dynamics.

Based on Mojeeb et al., 2017 observed a SEIR model on eradication of mosquito population and abolition outburst of malaria. Olaniyi et al., 2020 recommended a classification to validate the absence of a linear progression in the spread of malaria which agrees with Mandal et al., 2020 who envisioned a system to comprehend the malaria disease propagation. In another discourse, Bakary et al. (2018) suggested a model to analyse the impact of frequent biting of mosquitoes and blood transfusions. In another finding, the effects of immunization on malaria's underlying currents were studied by Rafia et al., 2018 and were reiterated by Mandal (2011), who provided a methodology to assess the fluctuation in the severity of the malaria epidemic by taking into account the cyclical impacts and mosquito bite frequency.

The existence of several classes of population is a factor that the majority of mathematical models for disease infection cases twitch from. A population of people with malaria plague is anticipated to follow the SEIR model, which is intended for the treatment of malaria (Mandal et al., 2011). The goal of mathematical models of malaria sickness, which are industrialized from a variety of angles and include the interaction between humans and mosquitoes in the model of malaria, is to eradicate the disease. Even in the worst-case scenario, it is expected that efforts to eradicate the disease will result in fewer deaths and illnesses overall than would occur if no action were taken (WHO, 2014). Consequently, anti-malarial drug fight occurs when impulsively arising mutants with

abridged drug vulnerability are provided with advantage to survive by the use of the anti-malarial. The frugal use of new anti-malarial drugs has been suggested to diminish the discerning pressure of parasite (Mackinnon, 2005). Alternatively, Mandal *et al.* (2011) argue that population, rather than individual-level interventions like many first-line therapies, such as the distribution of a real vaccine or insecticide-treated bed nets (ITNs), could prevent the outbreak of drug resistance.

The SEIR-SEI mathematical model guided Rwanda's malaria control efforts, providing guidance to policymakers as they developed a plan to lower infection rates and rein in the disease (Osman & Adu, 2017; Cai *et al.*, 2019). Furthermore, WHO (2019) notes that abolition of any disease is a determined aimed to achieve for smallpox and sanctioned diseases marks for extermination.

Abongi (2016) used the conventional Susceptible-Exposed-Infectious-Recovered (SEIR) human models and the Susceptible-Exposed-Infectious (SEI) vector mosquito models in Kenyan malaria models for assessing the influence of interferences in perfect controls. Also, WHO (2019) endorsed defensive treatment for the greatest at-risk malaria group such as expectant women have not been included in the study in control theory options in Kenya. According to DOMC (2010), there is no existing optimal control model for malaria interferences in Busia County, Kenya due to the country's diverse transmission zones. There is currently no optimal control model for four control variables in Busia County, Kenya that takes into account the IPTp malaria invasion research (WHO, 2014). This implies that the mathematical modelling of the host-vector model with SIRS_p in human population is crucial towards reducing the spread of malaria in Busia County, Kenya and appropriate awareness of such scientific tools is vital to avert the menace caused by the deadly disease.

III. Methodology

Model Development

Two populations are in play here; the human population in Busia County and the mosquito population in Busia County, where each of the populations has the tendency to influence the presence of malaria in the ecosystem. The interaction and migrations between the subpopulations are shown in the model description of figure (3.1). The directional arrows indicate migration from a subpopulation to another, the dashed non-directional lines indicate interactions without migration (clearly, human population cannot migrate into the mosquito subpopulation and vice versa). The human subpopulations are represented in the blue boxes while the mosquito subpopulations are represented in the red boxes.

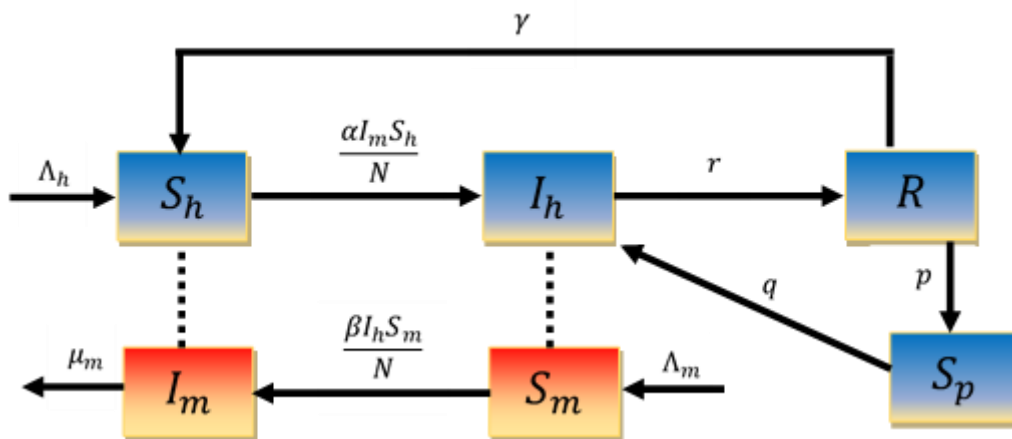


Figure 3.1: Model Description

The human population is divided into four subpopulations; the susceptible human subpopulation S_h , the infected human subpopulation I_h , the recovered human subpopulation R_h and the susceptible with plasmodium parasite human subpopulation S_p . The mosquito is subdivided into the infectious mosquito subpopulation I_m and the susceptible mosquito subpopulation S_m . The susceptible human subpopulation gets infected when there is an interaction with an infected mosquito with the force of infection

$$\frac{\alpha I_m S_h}{N}$$

where N is the total human population, α is the proportion of interaction that led to infection. The susceptible mosquitoes become infectious by interacting with the malaria-infected human subpopulation with the rate of infection

$$\frac{\beta I_h S_m}{M}$$

where β is the proportion of interaction that led to infection and M is the population of mosquitoes. The rate of influx into the susceptible human subpopulation and susceptible mosquito subpopulation are Λ_h and Λ_m respectively. An infected human recover from malaria at the rate r and it is assumed that a recovered human migrates to the susceptible human subpopulation at the rate γ . By writing out the rate of change of each subpopulation, the equations governing the malaria trend in the population is the system of equations (3.1) – (3.5).

$\frac{dS_h}{dt} = \Lambda_h + \gamma R - \frac{\alpha I_m S_h}{N}$	(3.1)
$\frac{dI_h}{dt} = \frac{\alpha I_m S_h}{N} - r I_h + q S_p$	(3.2)
$\frac{dS_p}{dt} = p R - q S_p$	(3.3)
$\frac{dR}{dt} = r I_h - \gamma R - p R$	(3.4)
$\frac{dS_m}{dt} = \Lambda_m - \frac{\beta I_h S_m}{M}$	(3.5)
$\frac{dI_m}{dt} = \frac{\beta I_h S_m}{M} - \mu_m I_m$	(3.6)

with the following initial conditions

$$\begin{cases} S_h(0) = S_h^0 > 0, \\ I_h(0) = I_h^0 \geq 0, \\ R_h(0) = R_h^0 \geq 0, \\ S_p(0) = S_{p,h}(0) \geq 0, \\ S_m(0) = S_m^0 > 0, \\ I_m(0) = I_m^0 \geq 0. \end{cases} \quad (3.7)$$

The parameters are also restricted to the following conditions

$$0 < \Lambda_h, \Lambda_m, \gamma, \alpha, \beta, r, \mu_m, p, q < 1, \quad (3.8)$$

Reproduction Numbers

The reproduction numbers are calculated by investigating the rate of change of the infectious class according to equations (3.2) and (3.6). Considering when a single infectious mosquito is brought into the susceptible human subpopulation, indicating that $I_m = 1$ and $S_h = N$, therefore equation (3.2) becomes

$$\frac{dI_h}{dt} = \alpha - r = r \left(\frac{\alpha}{r} - 1 \right).$$

By setting $R_{h,0} = \frac{\alpha}{r}$ as the reproduction number for the malaria infection in the human population, then

$$\frac{dI_h}{dt} = r(R_{h,0} - 1). \quad (3.9)$$

This shows that the infection in the human population dies out if $R_{h,0} < 1$ but remains endemic if $R_{h,0} > 1$. Similarly, when one malaria-infected human is brought into the population, where no mosquito is infectious, indicating that $I_h = 1$ and $S_m = M$, then equation (3.6) becomes

$$\frac{dI_m}{dt} = \beta - \mu_m = \mu_m \left(\frac{\beta}{\mu_m} - 1 \right). \quad (3.10)$$

By setting $R_{m,0} = \frac{\beta}{\mu_m}$ as the reproduction numbers for the mosquitoes to get infectious, then

$$\frac{dI_m}{dt} = \mu_m(R_{m,0} - 1). \quad (3.11)$$

Hence, if $R_{h,0} < 1$, then the mosquitoes do not become infectious.

Numerical Solution

The adaptive step-size method is used to solve the model equations (3.1) – (3.6). The method involves the adjustment of the step-size during numerical integration by taking note of the behaviour of the solution during each iteration. The Runge-Kutta-Fehlberg (RKF45) method is adopted in this study (see Amoo *et al.* (2022) and Montijano *et al.* (2024) for details). RKF45 smoothly combines Runge-Kutta of order 4 with order 5 by reducing the local truncation error. The problem under consideration can be written as

$$\frac{d}{dt} \mathbf{X} = \mathbf{F}(\mathbf{X}), \quad \mathbf{X}_0 = \mathbf{X}(t_0), \quad (3.12)$$

where $\mathbf{X} = (S_h, I_h, R_h, S_m, I_m)^T$. The RKF45 algorithm for the numerically solving the problem under consideration is as follows;

STEP 1: Initialise the step-size h_0 , time t_0 and the value of the variables X_0 .

STEP 2: Solve the problem with both Runge-Kutta of order 4 and of order 5. The RKF45 scheme is as follows;

$$\begin{aligned}
 K_1 &= hF(t_n, X_n), \\
 K_2 &= hF\left(t_n + \frac{h}{4}, X_n + \frac{1}{4}K_1\right), \\
 K_3 &= hF\left(t_n + \frac{3h}{8}, X_n + \frac{3}{32}K_1 + \frac{9}{32}K_2\right), \\
 K_4 &= hF\left(t_n + \frac{12h}{13}, X_n + \frac{1932}{2197}K_1 - \frac{7200}{2197}K_2 + \frac{7296}{2197}K_3\right), \\
 K_5 &= hF\left(t_n + h, X_n + \frac{439}{216}K_1 - 8K_2 + \frac{3680}{513}K_3 - \frac{845}{4104}K_4\right), \\
 K_6 &= hF\left(t_n + \frac{h}{2}, X_n - \frac{8}{27}K_1 + 2K_2 - \frac{3544}{2565}K_3 + \frac{1859}{4104}K_4 - \frac{11}{40}K_5\right), \\
 X_{n+1}^5 &= X_n^5 + \frac{25}{216}K_1 + \frac{1408}{2565}K_3 + \frac{2197}{4104}K_4 - \frac{1}{5}K_5. \\
 X_{n+1}^{5(*)} &= X_n^5 + \frac{16}{135}K_1 + \frac{6656}{12825}K_3 + \frac{28561}{56430}K_4 - \frac{9}{50}K_5 + \frac{2}{55}K_6.
 \end{aligned}$$

STEP 3: Estimate the local error

$$E = |X_{n+1}^5 - X_{n+1}^{5(*)}| \tag{3.13}$$

STEP 4: If $E < \text{tolerance}$, then X_{n+1}^5 is accepted as the solution at that time step and step-size for the next iteration is adjusted as

$$h_{n+1} = h_n \left(\frac{\text{tolerance}}{E}\right)^{\frac{1}{5}}. \tag{3.14}$$

Else, reject the solution and reduce h_n and repeat STEP 2

STEP 5: Repeat Steps 1 – 4 until the final time is reached.

Equilibrium points and stability

Consider the critical point of the equation (3.1) – (3.6) where all equations are equated to zero so that

$\Lambda_h + \gamma R - \frac{\alpha I_m S_h}{N} = 0$	(3.15)
$\frac{\alpha I_m S_h}{N} - r I_h + q S_p = 0$	(3.16)
$p R - q S_p = 0$	(3.17)
$r I_h - \gamma R - p R = 0$	(3.18)
$\Lambda_m - \frac{\beta I_h S_m}{M} = 0$	(3.19)
$\frac{\beta I_h S_m}{M} - \mu_m I_m = 0$	(3.20)

Disease-free equilibrium

Firstly, the disease-free equilibrium point can be found by setting $I_h = 0$ in all equations. To start with equation (3.19), we have

$$\Lambda_m - \frac{\beta \times 0 \times S_m}{M} = 0 \Rightarrow \Lambda_m = 0.$$

Next consider equation (3.18)

$$(r \times 0) - (\gamma + p)R = 0 \Rightarrow -(\gamma + p)R = 0 \Rightarrow R = 0.$$

Set $R = 0$ and $I_h = 0$ in equation (3.17) and (3.20) and we have

$$(p \times 0) - q S_p = 0 \Rightarrow -q S_p = 0 \Rightarrow S_p = 0.$$

$$\frac{\beta \times 0 \times S_m}{M} - \mu_m I_m = 0 \Rightarrow -\mu_m I_m = 0 \Rightarrow I_m = 0.$$

Equation (3.16) is automatically satisfied since $I_m = I_h = S_p = 0$. Substituting all the other variables into equation (3.15) gives

$$\Lambda_h + (\gamma \times 0) - \frac{\alpha \times 0 \times S_h}{N} = 0 \Rightarrow \Lambda_h = 0.$$

Hence, the disease-free equilibrium is therefore

$$(S_h^{DFE}, I_h^{DFE}, S_p^{DFE}, R^{DFE}, S_m^{DFE}, I_m^{DFE}) = (\xi, 0, 0, 0, \sigma, 0) \tag{3.21}$$

where $\Lambda_m = \Lambda_h = 0$ and ξ, σ are arbitrary values.

Other equilibrium points

However, other equilibrium points exist. We start by making R the subject from equation (3.18), we have

$$R = \frac{r}{\gamma + p} I_h. \tag{3.22}$$

From (3.19) and (3.20), we have

$$S_m = \frac{M\Lambda_m}{\beta I_h} \tag{3.23}$$

$$S_m = \frac{M\mu_m I_m}{\beta I_h}, \tag{3.24}$$

respectively. Hence, equating (3.23) and (3.24) implies

$$\frac{M\Lambda_m}{\beta I_h} = \frac{M\mu_m I_m}{\beta I_h} \Rightarrow I_m = \frac{\Lambda_m}{\mu_m}. \tag{3.25}$$

It is easy to see from equation (3.17) that

$$S_p = \frac{p}{q} R = \frac{pr}{q(\gamma + p)} I_h. \tag{3.26}$$

Looking at equation (3.16),

$$\begin{aligned} S_h &= \frac{N(rI_h - qS_p)}{\alpha I_m} \\ &= \frac{N\mu_m}{\alpha \Lambda_m} (rI_h - qS_p), \\ &= \frac{N\mu_m}{\alpha \Lambda_m} \left(rI_h - \frac{pr}{(\gamma + p)} I_h \right), \\ &= \frac{N\mu_m r}{\alpha \Lambda_m} \left(1 - \frac{p}{(\gamma + p)} \right) I_h. \end{aligned}$$

Hence,

$$S_h = \frac{N\mu_m r \gamma}{\alpha \Lambda_m (\gamma + p)} I_h. \tag{3.27}$$

Finally consider (3.15), we have

$$\begin{aligned} \Lambda_h + \gamma \left(\frac{r}{\gamma} I_h \right) - \frac{\alpha}{N} \left(\frac{\Lambda_m}{\mu_m} \right) \left(\frac{rN\mu_m \gamma}{\alpha \Lambda_m (\gamma + p)} I_h \right) &= 0 \\ \Lambda_h + rI_h - \frac{r\gamma}{(\gamma + p)} I_h &= 0. \\ \Lambda_h + \left(1 - \frac{\gamma}{(\gamma + p)} \right) rI_h &= 0. \\ \Lambda_h + \frac{pr}{(\gamma + p)} I_h &= 0. \end{aligned}$$

and therefore

$$I_h = - \frac{(\gamma + p)\Lambda_h}{pr}. \tag{3.28}$$

Since all parameters are greater than zero, then the $I_h < 0$. This is not physically possible and hence we say there are no other equilibrium point other than the disease-free equilibrium point.

Stability

The Jacobian of the system (3.1) – (3.6) is obtained by assembling the derivatives of the right-hand side of the equations with respect to all the variables S_h, I_h, S_p, R, S_m and I_m . The resulting matrix called the Jacobian is as follows;

$$\begin{pmatrix} -\frac{\alpha I_m}{N} & 0 & 0 & \gamma & 0 & -\frac{\alpha S_h}{N} \\ \frac{\alpha I_m}{N} & -r & q & 0 & 0 & \frac{\alpha S_h}{N} \\ 0 & 0 & -q & p & 0 & 0 \\ 0 & r & 0 & -\gamma - p & 0 & 0 \\ 0 & -\frac{\beta S_m}{M} & 0 & 0 & -\frac{\beta I_h}{M} & 0 \\ 0 & \frac{\beta S_m}{M} & 0 & 0 & \frac{\beta I_h}{M} & -\mu_m \end{pmatrix}.$$

The eigenvalues of the system can be found by solving the characteristic equation

$$\begin{vmatrix} -\frac{\alpha I_m}{N} - \lambda & 0 & 0 & \gamma & 0 & -\frac{\alpha S_h}{N} \\ \frac{\alpha I_m}{N} & -r - \lambda & q & 0 & 0 & \frac{\alpha S_h}{N} \\ 0 & 0 & -q - \lambda & 0 & 0 & 0 \\ 0 & r & 0 & -\gamma - p - \lambda & 0 & 0 \\ 0 & -\frac{\beta S_m}{M} & 0 & 0 & -\frac{\beta I_h}{M} - \lambda & 0 \\ 0 & \frac{\beta S_m}{M} & 0 & 0 & \frac{\beta I_h}{M} & -\mu_m - \lambda \end{vmatrix} = 0.$$

Evaluating the characteristic equation at the DFE by substituting $(S_h^{DFE}, I_h^{DFE}, S_p^{DFE}, R^{DFE}, S_m^{DFE}, I_m^{DFE}) = (\xi, 0, 0, 0, \sigma, 0)$,

gives;

$$\begin{vmatrix} -\lambda & 0 & 0 & \gamma & 0 & -\frac{\alpha \xi}{N} \\ 0 & -r - \lambda & q & 0 & 0 & \frac{\alpha \xi}{N} \\ 0 & 0 & -q - \lambda & 0 & 0 & 0 \\ 0 & r & 0 & -\gamma - p - \lambda & 0 & 0 \\ 0 & -\frac{\beta \sigma}{M} & 0 & 0 & -\lambda & 0 \\ 0 & \frac{\beta \sigma}{M} & 0 & 0 & 0 & -\mu_m - \lambda \end{vmatrix} = 0.$$

Evaluating the determinant along the first column gives

$$-\lambda \begin{vmatrix} -r - \lambda & q & 0 & 0 & \frac{\alpha \xi}{N} \\ 0 & -q - \lambda & 0 & 0 & 0 \\ r & 0 & -\gamma - p - \lambda & 0 & 0 \\ -\frac{\beta \sigma}{M} & 0 & 0 & -\lambda & 0 \\ \frac{\beta \sigma}{M} & 0 & 0 & 0 & -\mu_m - \lambda \end{vmatrix} = 0.$$

Further evaluating the determinant along the third column gives

$$-\lambda(-\gamma - p - \lambda) \begin{vmatrix} -r - \lambda & q & 0 & \frac{\alpha \xi}{N} \\ 0 & -q - \lambda & 0 & 0 \\ -\frac{\beta \sigma}{M} & 0 & -\lambda & 0 \\ \frac{\beta \sigma}{M} & 0 & 0 & -\mu_m - \lambda \end{vmatrix} = 0.$$

Even further evaluation of the determinant along the third column gives

$$\lambda^2(-\gamma - p - \lambda) \begin{vmatrix} -r - \lambda & q & \frac{\alpha \xi}{N} \\ 0 & -q - \lambda & 0 \\ \frac{\beta \sigma}{M} & 0 & -\mu_m - \lambda \end{vmatrix} = 0.$$

Finally, evaluate the determinant along the second row,

$$\lambda^2(-\gamma - p - \lambda)(-q - \lambda) \begin{vmatrix} -r - \lambda & \frac{\alpha \xi}{N} \\ \frac{\beta \sigma}{M} & -\mu_m - \lambda \end{vmatrix} = 0.$$

Which finally becomes

$$\begin{aligned} \lambda^2(-\gamma - p - \lambda) \left((\lambda + \mu_m)(r + \lambda) + \frac{\beta \alpha \sigma \xi}{MN} \right) &= 0. \\ \Rightarrow \lambda = 0, 0, -\gamma - p \text{ and } \lambda^2 + (r + \mu_m)\lambda + r\mu_m + \frac{\beta \alpha \sigma \xi}{MN} &= 0 \end{aligned} \tag{3.29}$$

Since $\alpha, \beta, M, N, \sigma, \xi, p, q > 0$, then the root of $\lambda^2 + (r + \mu_m)\lambda + r\mu_m + \frac{\beta\alpha\sigma\xi}{MN} = 0$ are all negative. Therefore, the DFE is always stable.

Parameter optimisation

Estimation of the most appropriate values for the parameters is important in the modelling of malaria due to the nature of the disease. Malaria is a non-communicable disease that requires two separate immiscible populations; hence, the next step is to estimate values for the parameters. The variable that can be easily obtained is the number of infected Kenyans and as such we optimise the parameters using the infected human population. In this case, the observed number of infected human population over a period of time is recorded in the vector $\mathbf{x}_0(t_k)$ while the model equations (3.1) – (3.6) is solved over the same time interval and the numerical result for the infected human population is stored in the vector $\mathbf{x}(t_k, \Theta)$ where $\Theta = (\Lambda_h, \Lambda_m, \gamma, \alpha, \beta, r, \mu_m)$ is the parameter vector which are to be optimised. The objective function is now written as

$$\text{minimise } \Theta = \sum_{k=1}^N |\mathbf{x}(t_k, \Theta) - \mathbf{x}_0(t_k)|^2. \quad (3.30)$$

The parameters, as stated in equation (3.8), are bounded in the interval $[0,1]$ and hence we set the bounds to the parameters as follows;

$$\begin{aligned} 0 < \Lambda_h < 1 \\ 0 < \Lambda_m < 1, \\ 0 < \gamma < 1, \\ 0 < \alpha < 1, \\ 0 < \beta < 1, \\ 0 < r < 1, \\ 0 < \mu_m < 1. \end{aligned}$$

The Broyden-Fletcher-Goldfarb-Shanno (BFGS) method is used to minimise the objective function. BFGS is a quasi-Newton method that iteratively approximates the inverse Hessian matrix in the search for the optimal solution (Xue *et al.*, 2022; Luo *et al.*, 2022). The update rule is set by the equation

$$B_{k+1} = B_k + \frac{(\Delta x_k)(\Delta x_k)^T}{(\Delta x_k)^T(\Delta s_k)} - \frac{B_k s_k s_k^T B_k}{s_k^T B_k s_k}$$

where B_k is the inverse Hessian matrix approximation, Δx_k is the gradients change and Δs_k is the change in the search parameter values and the search direction is

$$d_k = -B_k \nabla f(x_k).$$

The “minimize” function in Python SciPy contains the BFGS method and as such is used in this study to find the optimal values for the optimal parameters. The optimal values of the parameters are kept fixed while solving the model equations (3.1) – (3.6) and varying one parameter at a time to investigate the behaviour of the population under various conditions.

IV. Results

Simulation

The optimised parameters are substituted into the model equations as

$$\Lambda_h = 1, \gamma = 1, \alpha = 1, r = 0.39195362, \Lambda_m = 1, \beta = 1, \mu_m = 0.$$

To understand the response of each subpopulation to variation in the parameters, we say fix other parameters and vary one parameter.

Rate of human infection (α)

The susceptible human subpopulation gets infected when there is an interaction with an infected mosquito. The force of infection for the susceptible human subpopulation defined as

$$\frac{\alpha I_m S_h}{N},$$

is controlled by the value of α . Hence, variation in the rate of human infection is measured by the value of α . Figures (4.3) – (4.5) show the behaviour of the human subpopulations as the human infection rate increases. Figure (4.3) shows that the number of infected humans rises as the force of infection goes up. By increasing α , the proportion of interaction between infected mosquitoes and susceptible human also increases. Hence, more susceptible human gets infected and consequently leading to a rise in the infected human subpopulation, in agreement with the figure (4.3). The increase in the number of malaria-infected humans also raises the number of humans who migrate to the recovered class. Figure (4.4) shows the increase in the recovered subpopulation as α grows larger. Figure (4.5) shows a rise in the plasmodium-carrying human. As infected humans continue to rise,

there will be an accumulation of treated humans free of the symptoms, but still carry the plasmodium and as a result can get sick once their immunity deteriorates a little. However, the susceptible human subpopulation continues to drop as many humans are migrating into the infected class (see figure (4.6))

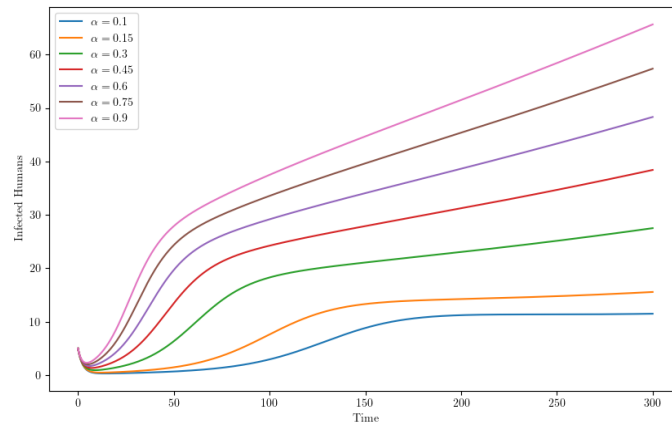


Figure Error! No text of specified style in document..1: Infected Humans as α increases

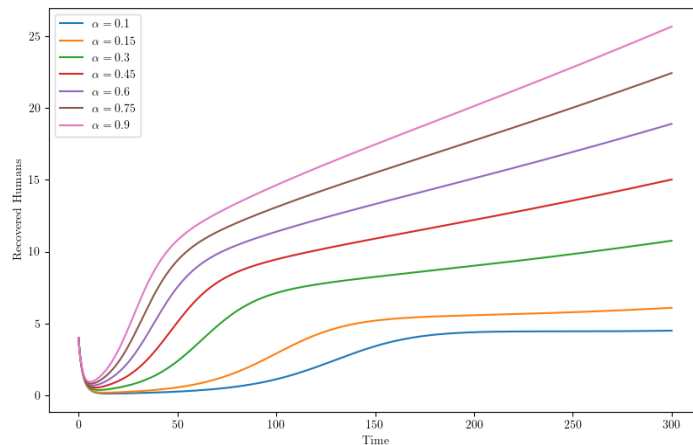


Figure Error! No text of specified style in document..2: Recovered human as α increases

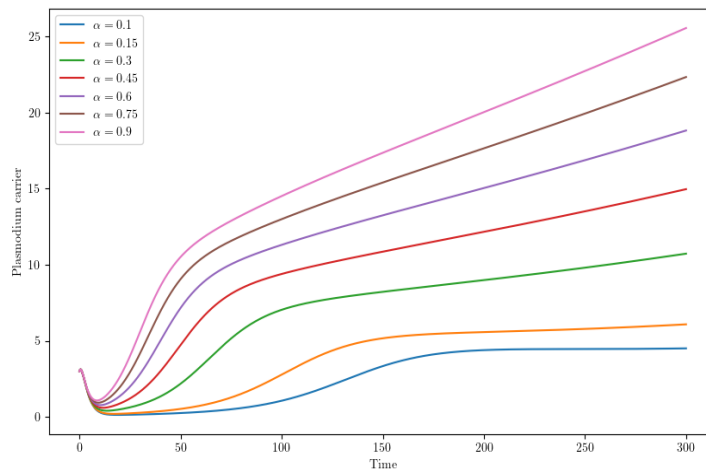


Figure Error! No text of specified style in document..3: Plasmodium carrier as α increases

Rate at which mosquitoes acquire the disease

Anopheles mosquitoes bite on a malaria-infected human to become infectious. The force at which the mosquitoes become infectious due to the interaction with malaria-infected human is defined as

$$\frac{\beta I_h S_m}{M},$$

and it is controlled by the value of β (the proportion of interaction that leading to infection). As the values of β is raised, the number of malaria-carrying mosquitoes is increased. This is well illustrated by the graph in figure (4.7). Increase in the number of mosquitoes that can infect human with malaria increase will definitely increase the number humans who get bitten by the mosquitoes and as a result increase the number humans who get infected with malaria. This is also illustrated by the graph of figure (4.8). The consequence of this will eventually be a reduction in the susceptible human subpopulation. Figure (4.9) shows the reduction in the susceptible human subpopulation as β goes up.

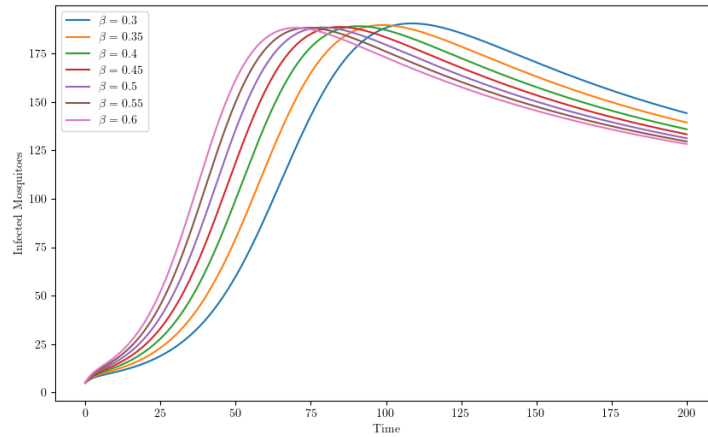


Figure Error! No text of specified style in document..4: Infected mosquitoes with β

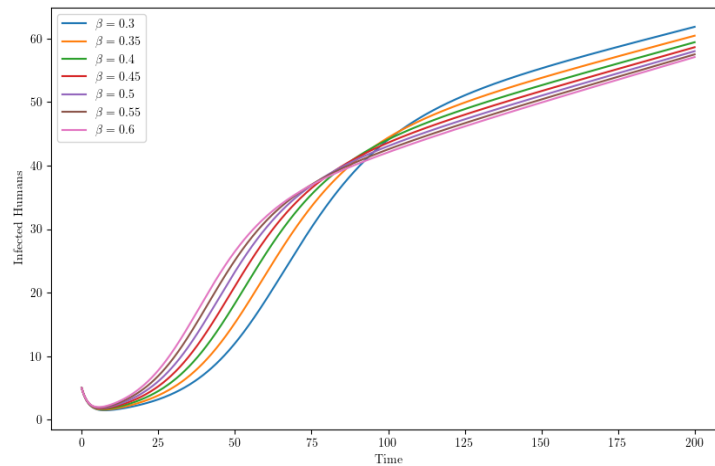


Figure Error! No text of specified style in document..5: Infected human with β

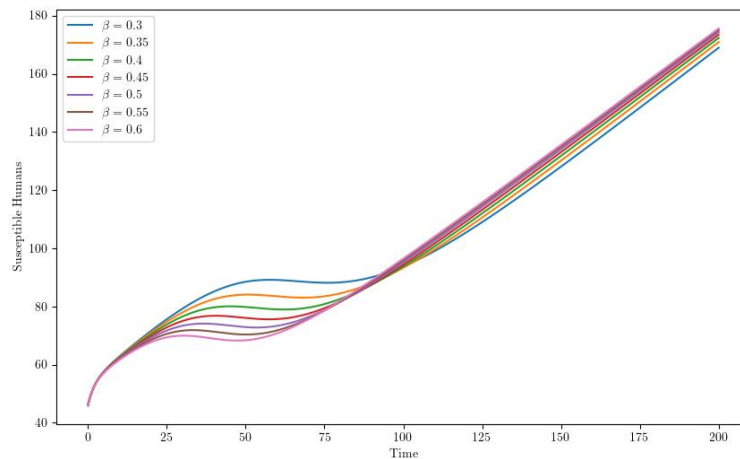


Figure Error! No text of specified style in document..6: Susceptible human with β

Rate of Recovery

Humans recover from malaria either by the ability of their immune system to fight it off or by the administration of anti-malarial drugs. The rate at which any human recovers (by any approach) is denoted as r . By increasing the rate of recovery from the malaria the number of infected humans reduces. Evidenced by the graph in figure (4.10), as malaria-infected humans recover faster, the number of infected humans reduce significantly. It can be observed that the rate of reduction in the infected human subpopulation also reduces as r increases (check the distance between the consecutive graphs in figure (4.10)). Due to the reduction in the infected human subpopulation, the exposure of mosquitoes to infected humans will reduce significantly and thereby ensuring that the infectious mosquito subpopulation reduces as r increases. This is typified in figure (4.11) where highest number of infectious mosquitoes occur at the lowest recovery rate r . Figure (4.12) shows the increase in the susceptible human subpopulation. This can be traced to the fact that a high percentage of recovered humans migrate to the susceptible class. Hence, an increase in the recovery rate r leads to migration of more humans into the susceptible human subpopulation.

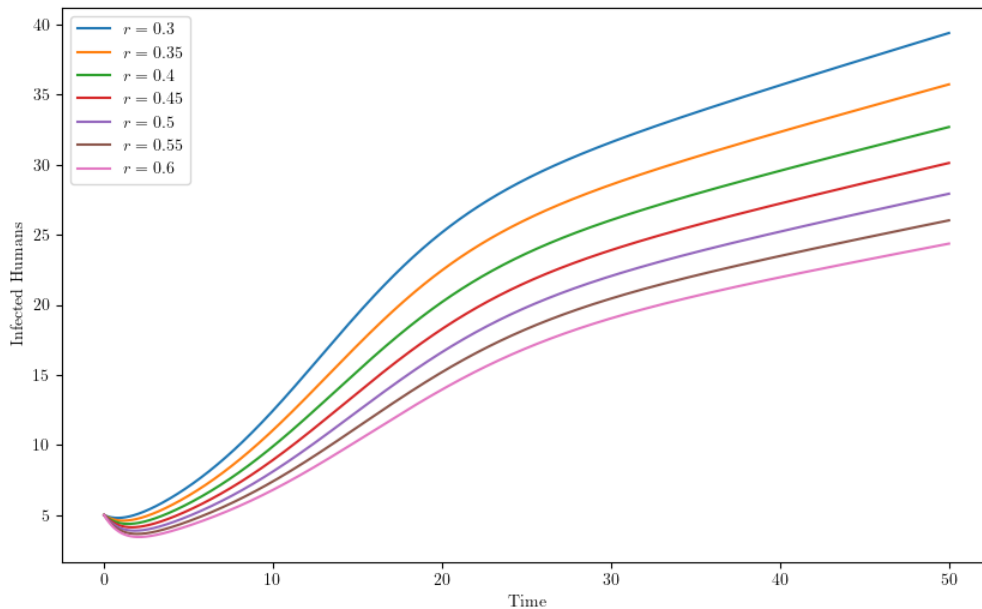


Figure Error! No text of specified style in document..7: Infected humans with r.

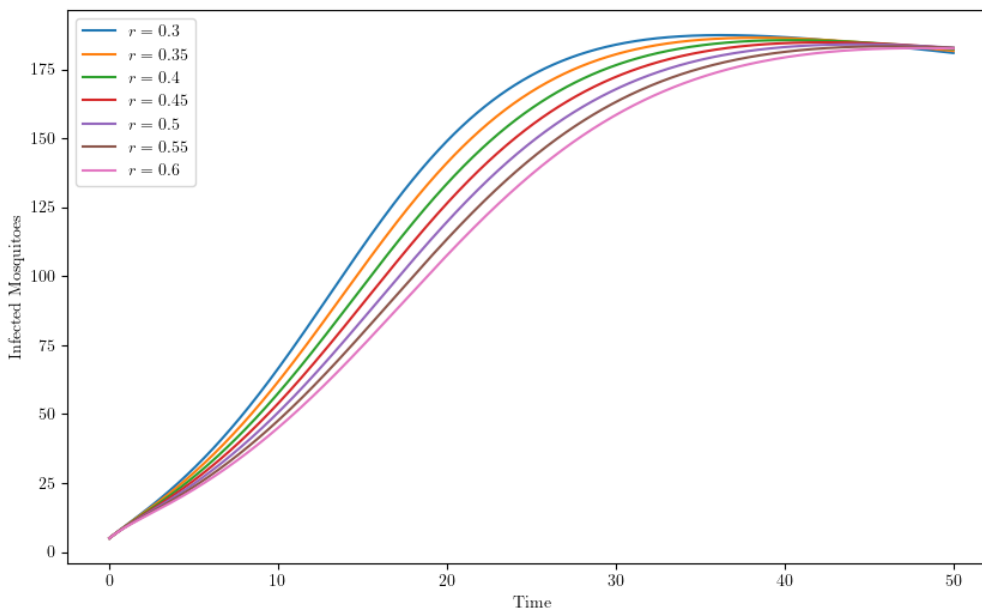


Figure Error! No text of specified style in document..8: Infected Mosquitoes with r.

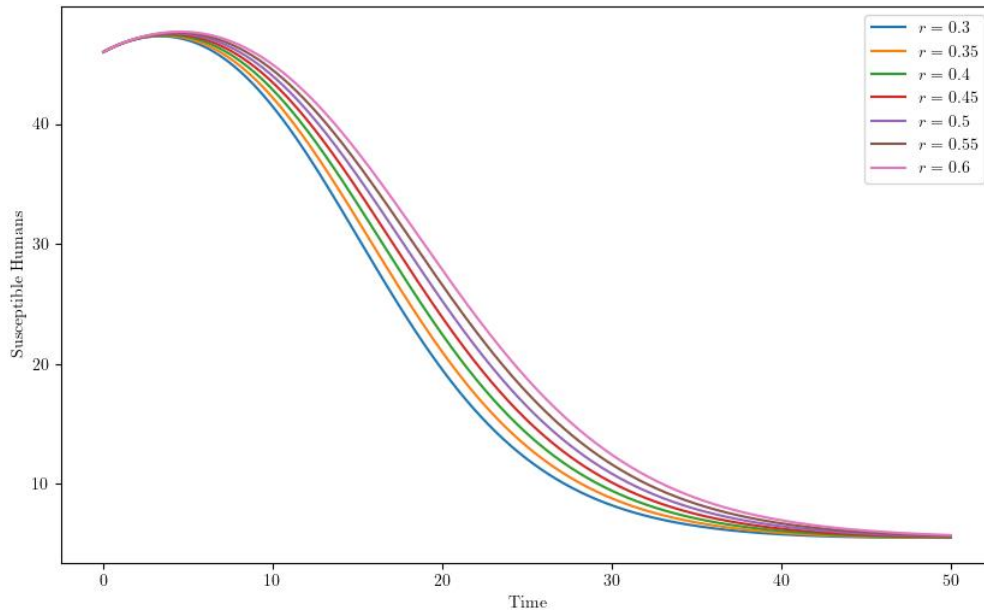


Figure Error! No text of specified style in document..9: Susceptible humans with r .

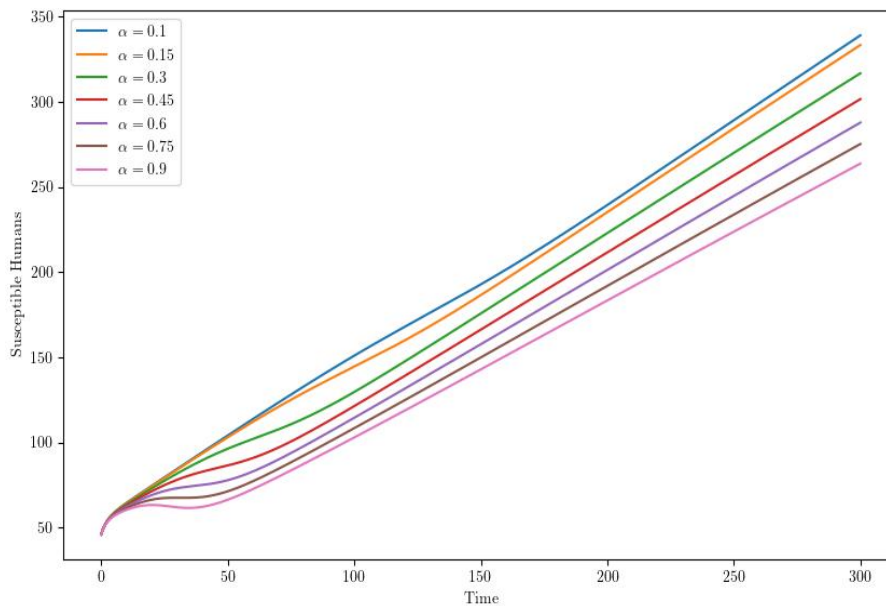


Figure Error! No text of specified style in document..10: Susceptible human as α increases

V. Discussion

By studying the numerical solution, the analysis showed that the number of infected humans rises while the susceptible human subpopulation reduces as the force of infection goes up. As the values of β is raised, the number of infectious mosquitoes increases, the number infected humans increases and the susceptible human subpopulation drops. Increase in the rate of recovery from malaria reduces the number of infected humans, the infectious mosquito subpopulation reduces and the susceptible human subpopulation increases.

VI. Conclusion

The model is very crucial in preventing the spread of malaria in Busia County, Kenya by finding the optimal values for the optimal parameters. The optimal values of the parameters were kept fixed and solved the model equations by varying one parameter at a time so as to investigate the behaviour of the population under various conditions. To understand the behaviour of each subpopulation by varying one parameter while the others are fixed.

References

- [1]. Abimbade, S. F., Olaniyi, S., & Ajala, O. A. (2022). Recurrent Malaria Dynamics: Insight From Mathematical Modelling. *The European Physical Journal Plus*, 137(3), 292.
- [2]. Abongo, B. (2019). *Malaria Vector Surveillance In The Context Of Enhanced Vector Control In Western Kenya* (Doctoral Dissertation, Liverpool School Of Tropical Medicine).
- [3]. Aldila, D. (2022). *Dynamical Analysis On A Malaria Model With Relapse Preventive Treatment And Saturated Fumigation*. *Computational And Mathematical Methods In Medicine*, 2022.
- [4]. Amoo, O. M., Fagbenle, R. O., & Oyewola, M. O. (2022). A Comparative Analysis Of Numerical Methods Applied To Nonsimilar Boundary Layer-Derived Infinite Series Equations. *Ain Shams Engineering Journal*, 13(5), 101713.
- [5]. Baihaqi, M. A., & Adi-Kusumo, F. (2020, September). Modelling Malaria Transmission In A Population With Seirsp Method. In *Aip Conference Proceedings* 2264(1). Aip Publishing.
- [6]. Cai, L. M., Li, Z., & Liu, J. (2019). Modeling And Analyzing Dynamics Of Malaria Transmission With Host Immunity. *International Journal Of Biomathematics*, 12(06), 1950074.
- [7]. Djidjou-Demasse, R., Abiodun, G. J., Adeola, A. M., & Botai, J. O. (2020). Development And Analysis Of A Malaria Transmission Mathematical Model With Seasonal Mosquito Life-History Traits. *Studies In Applied Mathematics*, 144(4), 389-411.
- [8]. Domc, (2010). *National Guidelines For Diagnosis, Treatment And Prevention Of Malaria In Kenya*, Division Of Malaria Control, Ministry Of Public Health And Sanitation, Nairobi, Kenya, 3rd Edition.
- [9]. Elnour, Z., Grethe, H., Siddig, K., & Munga, S. (2023). Malaria Control And Elimination In Kenya: Economy-Wide Benefits And Regional Disparities. *Malaria Journal*, 22(1), 117.
- [10]. Montijano, J. I., Rández, L., & Calvo, M. (2024). Explicit Runge–Kutta–Nyström Methods For The Numerical Solution Of Second Order Linear Inhomogeneous Ivps. *Journal Of Computational And Applied Mathematics*, 438, 115533.
- [11]. Olaniyi, S., & Obabiyi, O. S. (2013). Mathematical Model For Malaria Transmission Dynamics In Human And Mosquito Populations With Nonlinear Forces Of Infection. *International Journal Of Pure And Applied Mathematics*, 88(1), 125-156.